CHAPTER III

ELECTROMECHANICAL EFFECT IN CHOLESTERIC SAMPLES WITH FIXED BOUNDARY CONDITIONS: THEORETICAL ANALYSIS

3.1 Introduction

As explained in the previous chapter, chiral systems can sustain novel cross-couplings between fluxes and forces. The Lehmann rotation phenomenon is an unique example of cross-coupling between fluxes and forces in chiral systems. We also saw in the previous chapter that it is generally difficult to get cholesteric drops with zero azimuthal anchoring energy which is necessary to obtain the rotation phenomenon. This ideal situation can be realised only with a very special combination of chemicals. Since it is relatively easy to get samples with fixed boundary conditions using appropriately treated glass plates, it is desirable to develop techniques for observing the electromechanical effect in such samples. In this chapter we present a theoretical analysis of samples with fixed boundary conditions and subjected to both DC and AC electric fields.

3.2 DC field applied to a material with negative dielectric anisotropy

We first consider a material whose dielectric anisotropy in the untwisted state is negative, so that there is no dielectric realignment of the director under the action of the external field which is applied along the helical axis. This simplifies the .analysis considerably. As was shown in chapter II, the torque balance equation can be written as (see equation 2.15 in Sec.2.2)

$$\gamma_1 \frac{\partial \phi}{\partial t} = K_{22} \frac{\partial^2 \phi}{\partial z^2} + \nu_E E \tag{3.1}$$

This equation can be integrated to obtain a solution for ϕ by using appropriate boundary conditions. We now assume that a DC field is applied to a sample in which the director is fixed at both the boundaries $z = 0$ and d, where d is the thickness of the cell. In this case the medium has a static deformation. Equation (3.1) simplifies to

$$K_{22} \frac{\partial^2 \phi}{\partial z^2} + \nu_E E = 0 \tag{3.2}$$

Integrating this equation with respect to z, the solution is

$$\phi(z) = \frac{\phi_d z}{d} + \frac{\nu_E E z}{2K_{22}} (d - z) \tag{3.3}$$

where $\phi = 0$ and ϕ_d at z = 0 and d respectively. The director has a uniform twist in the sample in the absence of the applied field. When the field is applied, the variation of ϕ across the sample thickness becomes non-uniform as shown in figure 3.1. The thickness averaged value of ϕ can be calculated by integrating eqn. **(3.3)** with respect to z, i.e.,

$$\bar{\phi} = \frac{1}{d} \int_o^d \phi(z)\, dz$$

or

$$\bar{\phi} = \frac{\phi_d}{2} + \frac{\nu_E d^2 E}{12K_{22}}$$

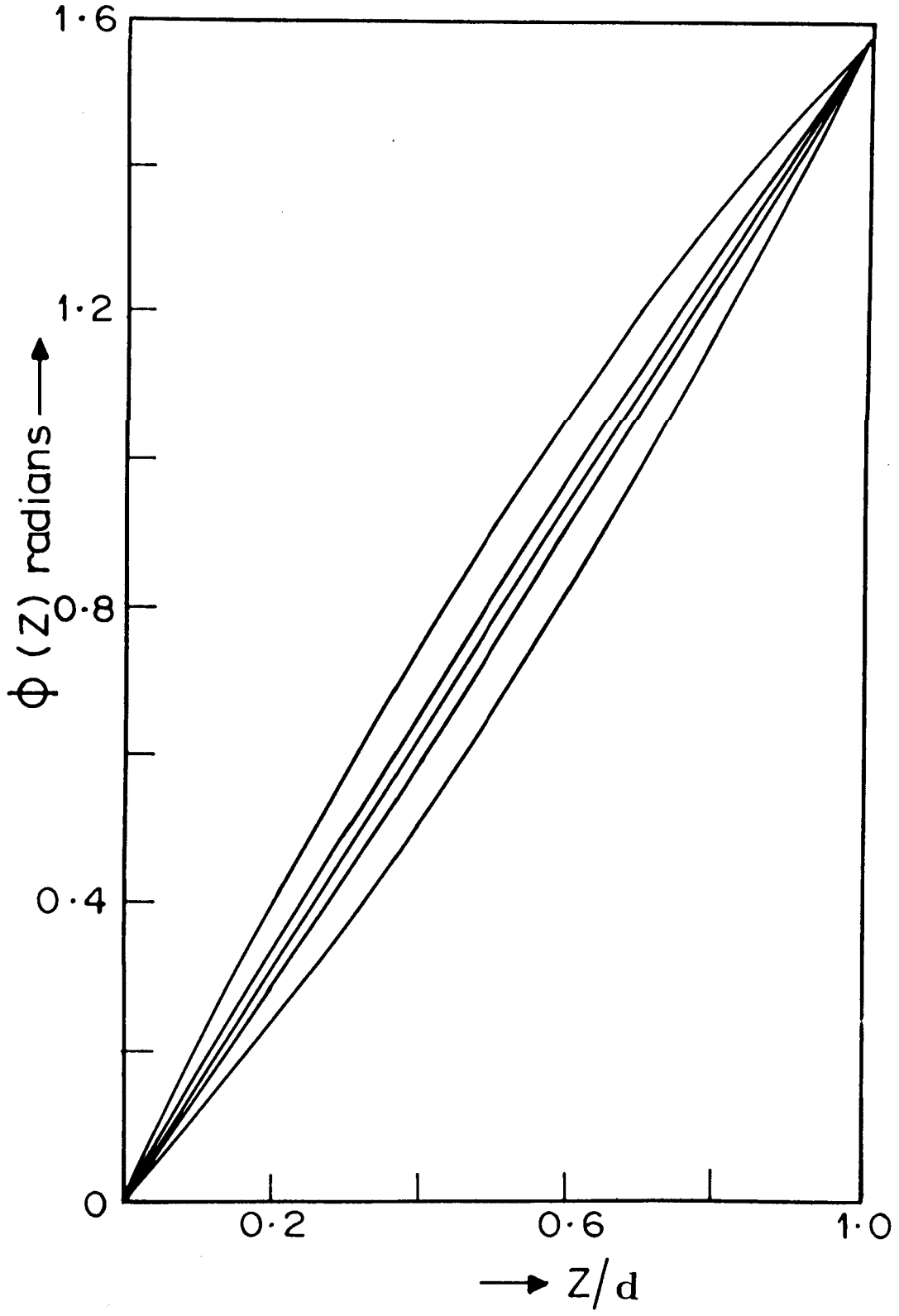

Figure 3.1. Theoretical $-profiles (from equation **3.3)** of the director in a $\pi/2$ twisted cholesteric cell subjected to a DC electric field. $\nu_E = 5\times10^{-5}NV^{-1}m^{-1}$, $K_{22} = 5\times10^{-12}$ newton, $d = 3\mu m$. The curves from top to bottom correspond to V = *$10* V, + 3V, 0 V, **-3** V and *-10* V respectively.

The thickness averaged value $\bar{\phi}$ will be greater than or less than that of the field-free value of $\phi_d/2$ depending on the sign of E (and that of ν_E), as seen in figure 3.1.

3.3 AC field applied to a material with negative dielectric anisotropy

It is usually preferable to apply an AC electric field rather than a DC electric field to liquid crystals to avoid electrolytic processes. The measurement of the electrooptic response is also easier with an **AC** field. If we choose a sample with negative dielectric anisotropy and apply an **AC** field, the corresponding torque produced due to the field will favour the director to be perpendicular to tlie field. However, in this case, above a certain threshold voltage, the field can produce an electrohydrodynamic instability in the medium (de Gennes, 1975). As this results in a convective flow in the medium, the electromechanical effect will be masked. Therefore here we restrict tlic applied voltage to values lower than the threshold for the formation of electrohydrodynamic instability. If tlie applied field is given by $E = E_o e^{i\omega t}$, one may expect in tlie linear regime that ϕ also oscillates with the frequency w. The time-dependent part of ϕ can be written as

$$\delta\phi(z,t) = \hat{\phi}(z)\, e^{i\omega t} \tag{3.4}$$

where $\hat{\phi}(z)$ is a complex amplitude. Substituting this in eqn. (3.1),

$$i\omega\phi\, e^{i\omega t} = \frac{K_{22}}{\gamma_1}\,\frac{\partial^2\phi}{\partial z^2}\, e^{i\omega t} + \frac{\nu_E E_o}{\gamma_1}\, e^{i\omega t}$$

i.e.,

$$\frac{K_{22}}{\omega\gamma_1}\,\frac{\partial^2\phi}{\partial z^2} - i\phi = -\frac{\nu_E E_o}{\omega\gamma_1} \tag{3.5}$$

This is a second order differential equation in ϕ , and the general solution for the complex amplitude is of the form

$$\begin{aligned}\hat{\phi}(z) &= c_1 e^{(1+i)pz} + c_2 e^{-(1+i)pz} - \frac{i\nu_E E_o}{\omega\gamma_1} \\ &= a \cos h\, p(1+i)\, z + b \sin h\, p(1+i)\, z - \frac{i\nu_E E_o}{\omega\gamma_1} \qquad (3.6)\end{aligned}$$

where a $= c_1 + c_2$ and $b = c_1 - c_2$ and $p = \sqrt{\omega\gamma_1/2K_{22}}$

Using the boundary conditions

$$\hat{\phi}(o) = 0 \quad \text{and} \quad \hat{\phi}(d) = 0$$

the explicit expression for the amplitude is given by

$$\begin{aligned}\hat{\phi}(z) &= \left[-\left(\frac{\nu_E E_o}{\omega\gamma_1}\right)\{\sin pz \sinh pz - (\cos pd + \cosh pd)^{-1}\right. \\ &\quad \times(\sinh pd \sin pz \cosh pz + \sin pd \cos pz \sinh pz)\} \\ &\quad + i\left[\left(\frac{\nu_E E_o}{\omega\gamma_1}\right)\left\{\cos pz \cosh pz - (\cos pd + \cosh pd)^{-1}\right.\right. \\ &\quad \left.\left.\times(\sinh pd \cos pz \sinh pz - \sin pd \sin pz \cosh pz) - 1\right\}\right] \qquad (3.7)\end{aligned}$$

Wc liavc shown the real and imaginary parts of $\phi(z)$ for two different frequencies in fig. (3.2). The lower frequency corresponds to $\frac{\nu_E E_o}{\omega\gamma_1} \simeq 0.86$ and the higher one to 0.086. It is clear that as the frequency increases, the amplitude decreases while the phase lag with respect to the applied field increases.

When an AC field is applied to a liquid crystal with negative dielectric anisotropy, the director prefers to be perpendicular to the field. A convenient way of detecting changes in the director profile is by using an optical technique. However, in a

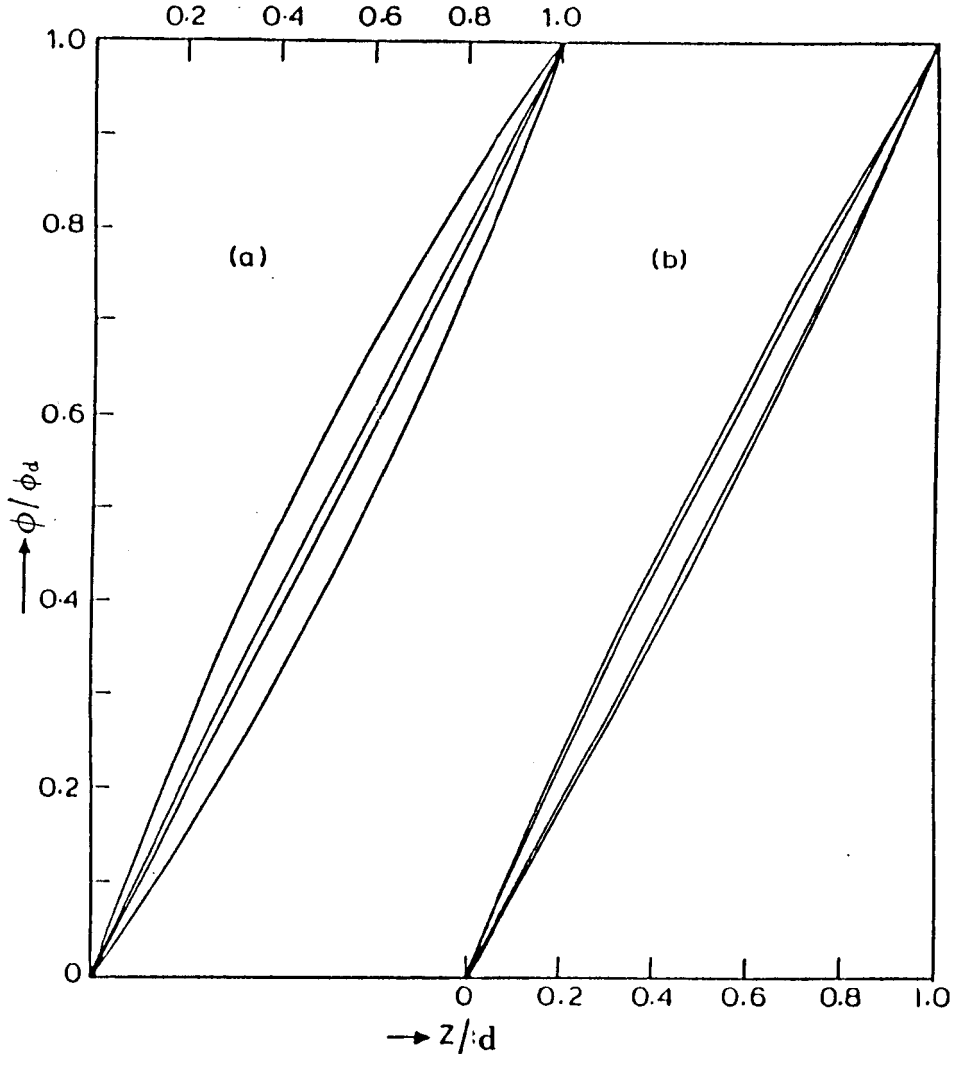

Figure 3.2. Theoretical curves showing the real and imaginary components of the field dependent amplitude $\hat{\phi}/\phi_d$ (from eqn.3.7) superposed on the uniform field free azimuthal profile. d=3μm, K_{22}=5×$10^{-12}N$. (a) $w\gamma_1$ = 0.7 Nm^{-2}. The first and third curves from the top (bottom) correspond to the real and imaginary parts of $\hat{\phi}/\phi_d$ for $\nu_\xi E_o$=0.6(-0.6)Nm^{-2} respectively. (b) $w\gamma_1$=7Nm^{-2}. The first and third curves from the top (bottom) correspond to the imaginary and real parts of ϕ/ϕ_d for $\nu_\xi E_o$ = -0.6(+0.6)Nm^{-2} respectively.

chiral nematic made of the usual materials and for typical sample thicknesses, the optical phase difference of the sample is much larger than the angle of twist. In such a case, the polarisation of an incident parallel light beam follows the director (Mauguin limit) and the deformation in +-profile cannot be detected optically by using a beam of light passing along the helical axis (see for e. g., de Gennes, 1975). But the avcragc azimuthal angle of the distorted director field for a material with negative $\Delta\epsilon$ can be sensed using light beams propagating at a large angle to the helical axis. We describe in chapter IV the use of conoscopy for this purpose.

3.4 AC field applied to a material with positive dielectric anisotropy

The optical problem can also be overcome by using a material which has *positive* dielectric anisotropy in the untwisted state. When an AC field is applied to tlie sample so that the applied voltage is above the threshold for the Freedericksz transition, a tilt-deformation is produced in the director field thus reducing the effective birefringence of the sample. This reduces the total phase difference introduced by the cell. It is then possible to avoid the problem discussed above and to detect the changes in the $\phi(z)$ profile.

The thickness of the sample also plays a crucial role when using materials with positive $\Delta\epsilon$. It is necessary to select a sample thickness $d < \frac{P}{4}$, where P is the pitcli of the cholesteric helix. For larger thicknesses the helical axis rotates to the XY plane above a threshold voltage (Chigrinov et al., 1979) giving rise to a striped domain pattern. Also if $\Delta\epsilon$ is very large, the Freedericksz transition occurs at a very low voltage. The average orientation of the director in tlie sample tilts towards tlie field as the voltage is increased above the threshold and the effect of the electromechanical

coupling becomes weaker. Since the torque due to this coupling is linear in E (see equation 3.1), it is better to apply higher voltages to the cell to improve the possibility of detecting the corresponding signal. However, we cannot make $\Delta\epsilon$ too small as the sample becomes unstable to a flexoelectric periodic distortion if $\Delta\epsilon \approx 0$ (Bobylev *et* al., 1977).

From the above discussion, we can expect to get an electrooptic signal due to the electromechanical coupling if a material with weakly positive dielectric anisotropy is chosen and the pitch and sample thickness are properly adjusted.

We consider a cholesteric liquid crystal sample with a natural helical wavevector q taken between two conducting glass plates separated by a gap d (Fig.3.3). As in the previous section, the lower plate is treated for an alignment of the director in the plane of the plate along the X-axis. The upper plate is treated for an alignment along a direction making an azimuthal angle ϕ_d with respect to the X-axis. The material has a positive dielectric anisotropy $\Delta\epsilon = \epsilon_{\parallel} - \epsilon_{\perp}$. Here we ignore the small biaxiality of the cholesteric medium. When we apply an AC electric field at a frequency f between the two conducting plates, the azimuthal profile becomes non-uniform and oscillates at the frequency f because of the electromechanical coupling ν_E. We note that in the present geometry there is no contribution to the orientation of the director from the other independent electromechanical coefficient (de Gennes, 1975).

In a positive dielectric anisotropy material, the distortion of the director pattern brought about by the electric field can induce an electric polarisation due to flexoelectric effects. Our electrooptic experiments (see Chapter IV) have shown that there is no significant flexoelectric contribution to the signal. We have neglected this contribution in our theoretical model. In principle the anisotropy of conductivity

can produce space charges in a distorted director field. We have ignored this effect also for the sake of simplicity.

There is no threshold for the distortion due to electromechanical effect as it changes linearly with the applied electric field E. As we have already discussed, at low voltages, this distortion is not detectable optically because of the strong anchoring conditions at the two boundaries with a parallel beam of light. As the applied field is increased beyond the Freedericksz threshold value, the director field develops a tilt distortion. The components of the director in the XYZ coordiriate system (Fig.3.3) are

$$\hat{n} \square (\cos\theta \cos\phi, \cos\theta \sin\phi, \sin\theta) \tag{3.8}$$

Both θ and ϕ are functions of the z-coordinate. The elastic energy density of the distorted medium is given by

$$F_d = \frac{K_{11}}{2}(div\,\hat{n})^2 + \frac{K_{22}}{2}(\hat{n} \cdot curl\,\hat{n} - q)^2 + \frac{K_{33}}{2}(\hat{n} \times curl\,\hat{n})^2 \tag{3.9}$$

where K_{11}, K_{22} and K_{33} are the splay, twist and bend elastic constants respectively. The dielectric energy density is

$$F_{diel} = -\frac{\Delta\epsilon}{8\pi}(\hat{n} \cdot \vec{E})^2 \,. \tag{3.10}$$

The field is applied along the z-direction, i.e., E = E,. For the sake of simplicity, we assume that tlie medium is free of ionic impurities, i.e,

$$div\ D = 0 \tag{3.11}$$

where D is the dielectric displacement vector.

Since variations occur only along the z-direction, we get $\frac{}{\mathrm{dz}} - 0$ or D, = constant, where

$$D_z = \epsilon_\perp E_z + \mathrm{A}\epsilon n_z^2 E_z \tag{3.12}$$

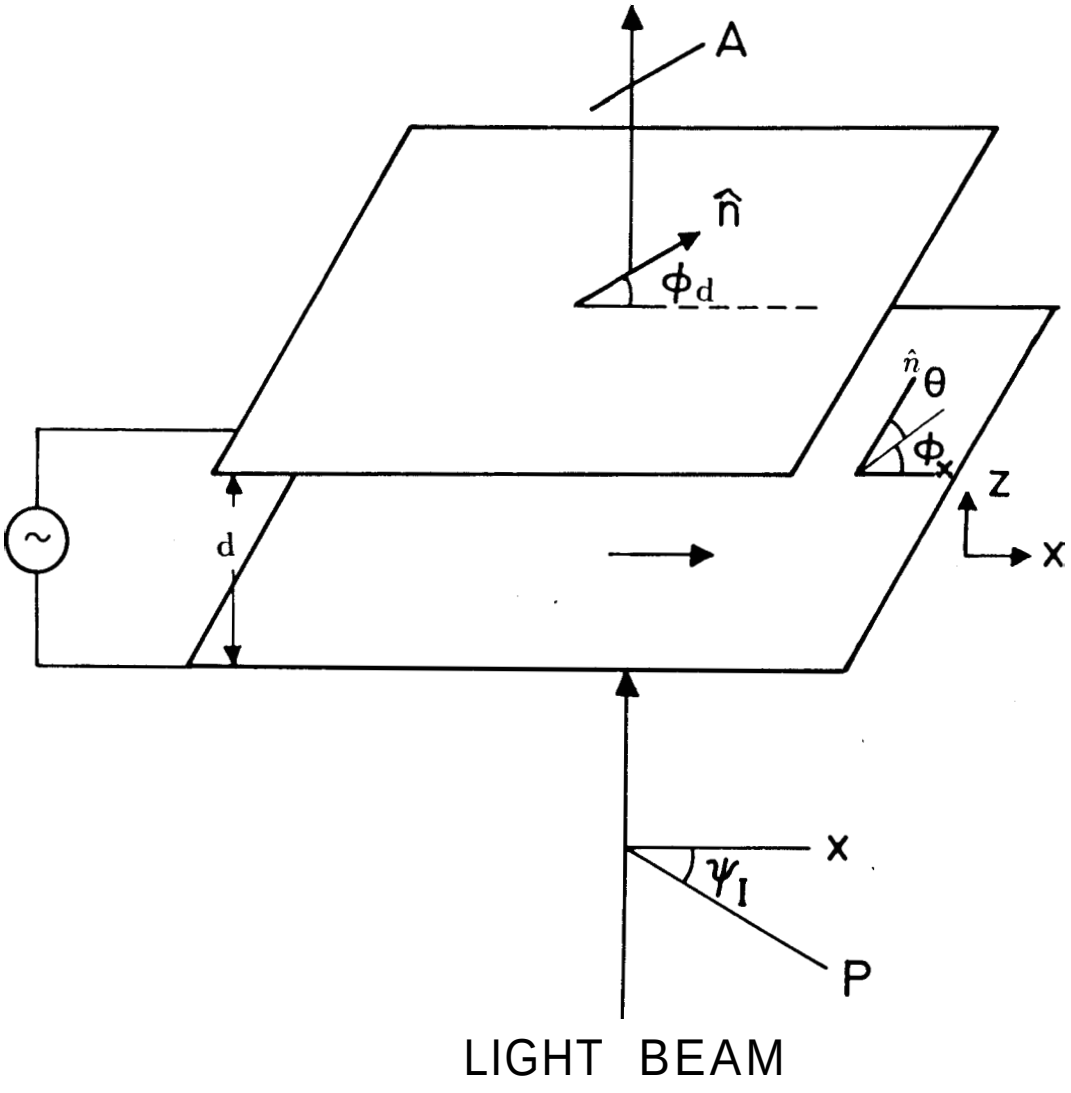

Figure 3.3. Schematic diagram of the geometry considered in section **3.4.** P and *A* are polarizer and analyzer respectively.

$$E_z = \frac{D_z}{(\epsilon_\perp + \Delta\epsilon n_z^2)} \tag{3.13}$$

The voltage across the sample is

$$V = \int_o^d E_z\, dz = D_z \int_o^d \frac{dz}{(\epsilon_\perp + \Delta\epsilon n_z^2)} \tag{3.14}$$

The molecular field corresponding to the elastic and dielectric energy densities are obtained by using the relation

$$h_\alpha = -\frac{\partial F}{\partial n_\alpha} + \frac{\partial}{\partial z}\left[\frac{dF}{d(\partial n_\alpha/\partial z)}\right] \tag{3.15}$$

Using this equation the X, Y and Z components of the molecular field corresponding to the elastic energy are given by

$$\begin{aligned} h_x^{el} = {} & K_{22}\left[-2n_x\left(\frac{\partial n_y}{\partial z}\right)^2 + 2n_y \frac{\partial n_x}{\partial z}\frac{\partial n_y}{\partial z} + n_y^2 \frac{\partial^2 n_x}{\partial z^2}\right. \\ & \left. - n_x n_y \frac{\partial^2 n_y}{\partial z^2} - 2q \frac{\partial n_y}{\partial z}\right] \\ & + K_{33}\left[n_x\left\{\left(\frac{\partial n_x}{\partial z}\right)^2 + \left(\frac{\partial n_y}{\partial z}\right)^2\right\} + 2n_z \frac{\partial n_x}{\partial z}\frac{\partial n_z}{\partial z}\right. \\ & \left. + n_x^2 \frac{\partial^2 n_x}{\partial z^2} + n_x n_y \frac{\partial^2 n_y}{\partial z^2} + n_z^2 \frac{\partial^2 n_x}{\partial z^2}\right] \end{aligned} \tag{3.16}$$

$$h_y^{el} = K_{22}\left[-2n_y\left(\frac{\partial n_x}{\partial z}\right)^2 + 2n_x\frac{\partial n_x}{\partial z}\frac{\partial n_y}{\partial z} + n_x^2\frac{\partial^2 n_y}{\partial z^2}\right.$$

$$\left. -n_x n_y\frac{\partial^2 n_x}{\partial z^2} + 2q\ \frac{\partial n_x}{\partial z}\right]$$

$$+K_{33}\left[n_y\left\{\left(\frac{\partial n_x}{\partial z}\right)^2 + \left(\frac{\partial n_y}{\partial z}\right)^2\right\} + 2n_z\ \frac{\partial n_y}{\partial z}\ \frac{\partial n_z}{\partial z}\right.$$

$$\left. +n_x n_y\frac{\partial^2 n_x}{\partial z^2} + (n_y^2 + n_z^2)\frac{\partial^2 n_y}{\partial z^2}\right] \qquad (3.17)$$

and

$$h_z^{el} = \left[K_{11}\frac{\partial^2 n_z}{\partial z^2} - K_{33}\,n_z\left\{\left(\frac{\partial n_x}{\partial z}\right)^2 + \left(\frac{\partial n_y}{\partial z}\right)^2\right\}\right] \qquad (3.18)$$

In order to calculate the dielectric contribution to the molecular field, we note that as $\vec{\nabla} \times \vec{E} = 0$,

$$\frac{\partial E_x}{\partial z} = \frac{\partial E_z}{\partial x}$$

But at the plates $\frac{}{ax} - 0$. Hence E_x = constant which should be zero on the conducting plate.

Hence from equation (3.10),

$$h_x^{diel} = 0 \qquad (3.19)$$

and similarly $E_y = 0$ and

$$h_y^{diel} = 0 \qquad (3.20)$$

Finally from equation (3.10),

$$F^{diel} = -\frac{\Delta\epsilon}{8\pi}E_z^2 n_z^2 \qquad (3.21)$$

and $$h^{e} = \frac{\Delta\epsilon}{4\pi}E_z^2 n_z \qquad (3.22)$$

The molecular field due to the electromechanical coupling is given by (see equation 2.5)

$$h^{EM} = \nu_E \hat{n} \times \vec{E} \tag{3.23}$$

The components of this molecular field are

$$h_x^{EM} = \nu_E n_y E_z \tag{3.24}$$

$$h_y^{EM} = -\nu_E n_x E_z \tag{3.25}$$

$$h_z^{EM} = 0 \tag{3.26}$$

The hydrodynamic contribution to the molecular field is given by

$$h_\mu = \gamma_1 N_\mu + \gamma_2 n_\alpha A_{\alpha\mu} \tag{3.27}$$

where

$$\vec{N} = \dot{n} - \omega \times \hat{n},$$

$$\vec{\omega} = \frac{1}{2} curl\, \vec{V},$$

$$\text{and} \quad A_{\alpha\beta} = \frac{\partial_\alpha V_\beta + \partial_\beta V_\alpha}{2}$$

In considering the hydrodynamic contribution, for the sake of sirriplicity, we ignore all velocities and take into account only the rotational motion of the director. We then get

$$h_\alpha^{hydro} = \gamma_1 \dot{n}_\alpha$$

The three components of the molecular field are

$$h_x^{hydro} = \gamma_1 \dot{n}_x \tag{3.28}$$

$$h_y^{hydro} = \gamma_1 \dot{n}_y \tag{3.29}$$

$$h_z^{hydro} = \gamma_1 \dot{n}_z \tag{3.30}$$

Here the dot represents the time derivative and γ_1 is the rotatiorial viscosity constant (de Gennes, 1975). We can now write the torque balance relations taking into account the molecular fields due to all the processes listed above, i.e., with $\Gamma = \hat{n} \times \vec{h}$,

$$\Gamma^{el} + \Gamma^{diel} + \Gamma^{EM} - \Gamma^{hydro} = 0 \tag{3.31}$$

There are only two independent torque balance relations for the director. Following the procedure given by Bodenschatz *et* al. (1988) we write the two independent components of the torque as follows:

$$\Gamma_2 = \sin\theta (h, \cos\phi + h_y \sin\phi) - h_z \cos\theta = 0 \tag{3.32}$$

and

$$\Gamma_3 = -h_x \sin\phi + \mathrm{h}, \cos\phi = 0 \tag{3.33}$$

where the x-component of the total molecular field h_x arising from the elastic (from equation 3.16), dielectric (from equation 3.19), the electromechanical (from equation 3.24) and hydrodynamic contributions (from equation 3.28) is given by

$$\begin{aligned} h_x \;=\; & K_{22}\left[-2n_x\left(\frac{\partial n_y}{\partial z}\right)^2 + 2n_y \frac{\partial n_x}{\partial z}\frac{\partial n_y}{\partial z} + n_y^2 \frac{\partial^2 n_x}{\partial z^2}\right. \\ & \left. -n_x n_y \frac{\partial^2 n_y}{\partial z^2} - 2q \frac{\partial n_y}{\partial z}\right] \\ & + K_{33}\left[n_x\left\{\left(\frac{\partial n_x}{\partial z}\right)^2 + \left(\frac{\partial n_y}{\partial z}\right)^2\right\} + 2n_z \frac{\partial n_x}{\partial z}\frac{\mathrm{dn},}{\partial z} + n_x^2 \frac{\mathrm{d^2n},}{\partial z^2}\right. \\ & \left. + n_x n_y \frac{\partial^2 n_y}{\partial z^2} + n_z^2 \frac{\partial^2 n_x}{\partial z^2}\right] + \frac{\nu_E n_y D_z}{(\epsilon_\perp + \Delta\epsilon n_z^2)} - \gamma_1 \dot{n}_x \end{aligned}$$

where equation (3.13) has been used for E,.

Similarly using equations (3.17), (3.20), (3.25) and (3.29) the y-component of the total molecular field is given by

$$h_y = K_{22}\left[-2n_y\left(\frac{\partial n_x}{\partial z}\right)^2 + 2n_x \frac{\partial n_x}{\partial z}\frac{\partial n_y}{\partial z} + n_x^2 \frac{\partial^2 n_y}{\partial z^2}\right.$$

$$\left. -n_x n_y \frac{\partial^2 n_x}{\partial z^2} - 2q \frac{\partial n_x}{\partial z}\right]$$

$$+K_{33}\left[n_y\left\{\left(\frac{\partial n_x}{\partial z}\right)^2 + \left(\frac{\partial n_y}{\partial z}\right)^2\right\} + 2n_z \frac{\partial n_y}{\partial z}\frac{\partial n_z}{\partial z} + n_x n_y \frac{\partial^2 n_x}{\partial z^2}\right.$$

$$\left. +(n_y^2 + n_z^2)\frac{\partial^2 n_y}{\partial z^2}\right] - \frac{\nu_E n_x D_z}{(\epsilon_\perp + \Delta\epsilon n_z^2)} - \gamma_1 \dot{n}_y$$

Similarly using equations (3.18), (3.22), (3.26) and (3.30) the z-component of the total molecular field h, is given as

$$h_z = \left[K_{11}\frac{\partial^2 n_z}{\partial z^2} - K_{33} n_z\left\{\left(\frac{\partial n_x}{\partial z}\right)^2 + \left(\frac{\partial n_y}{\partial z}\right)^2\right\}\right]$$

$$+\frac{\Delta\epsilon}{4\pi}\frac{D_z^2 n_z}{(\epsilon_\perp + \Delta\epsilon n_z^2)} - \gamma_1 \dot{n}_z$$

Using these molecular field components and the components of the director given in equation (3.8) after simplification we get

$$\Gamma_2 = (K_{11} - K_{33}) \sin\theta \cos\theta \left(\frac{\partial\theta}{\partial z}\right)^2$$

$$+\{K_{33}(\cos 28) - 2K_{22}\cos^2\theta\} \sin\theta \cos\theta \quad (2)^2$$

$$-(K_{11}\cos^2 8 + K_{33}\sin^2 8)\frac{\partial^2 8}{\partial z^2} - 2y\, K_{22} \sin\theta \cos 8 \frac{\partial\phi}{\partial z}$$

$$-\frac{\mathbf{At}}{4\pi}\frac{D_z^2 \sin 0 \cos 0}{(\epsilon_\perp + \Delta\epsilon \sin^2 \theta)^2} + \gamma_1\dot{\theta} = 0 \tag{3.34}$$

and

$$\begin{aligned}\Gamma_3 \;=\; & (K_{33}\sin^2\theta + K_{22}\cos^2\theta)\cos\theta\left(\frac{\partial^2\phi}{\partial z^2}\right) \\ & +2(K_{33}\cos 2\theta - 2K_{22}\cos^2\theta)\sin\theta\left(\frac{\partial\theta}{\partial z}\right)\left(\frac{\partial\phi}{\partial z}\right) \\ & -2K_{22}q\sin 0\frac{\partial\theta}{\partial z} - \frac{\nu_E D_z \cos \mathbf{e}}{(\epsilon_\perp + \mathbf{At}\sin^2 0)} \\ & -\gamma_1\cos\theta(\dot{\phi}) = 0\end{aligned} \tag{3.35}$$

where equation *(3.13)* has been used for E_z.

The above relations rcducc in the static limit to those derived by Leslie (1971) when $\nu_E = 0$. If an AC field at a frequency f is applied to the cell, we can write

$$D_z = D_{zo}\sin 2\pi f t \tag{3.36}$$

If the cell thickness d is less than $P/4$, the medium can be expected to be untwisted. The fixed boundary conditions can then be written as

$$\theta(0,t) = \phi(0,t) = \theta(d,t) = \phi(d,t) = 0 \tag{3.37}$$

Equations **(3.34)** and *(3.35)* are coupled non-linear partial differential equations in 0 and ϕ. 0 would remain zero for a material with negative dielectric anisotropy and these equations would reduce to those that we have already discussed in Section *3.3.*

$\theta \neq 0$ in the present case and θ and ϕ get strongly coupled through the q -dependent terms in equations (3.34) and (3.35). We have tried to solve these equations using the DPDES subroutine of the IMSL library. We found that the program was not very efficient for this purpose and it took a very long computation time to solve the equations. In fact, we could only make calculations by dividing the thickness of the sample and tlie time period of tlie applied AC signal to only 41 equal parts. We used the following material parameters which are typical values for a room temperature nematic:

$$K_{11} = 1.4 \times 10^{-11} N,\ K_{22} = 1.0 \times 10^{-11} N,\ K_{33} = 3 \text{ x } 10^{-11} N,$$

$$\gamma_1 = 0.07 N s m^{-2},\ \epsilon_\perp = 4,\ \Delta\epsilon = 1.0 \text{ and } \nu_E = 0.5 \text{ x } 10^{-5} q_O\ N/V m^2.$$

The sample thickness d used in these theoretical calculations was $3\mu m$ which is a typical value used in our experiments to be discussed in the next chapter. Some illustrative calculations have been made at frequency f=18 I-Iz and D_{zo}=9.36x$10^6 V/m$ for a few different values of q (and hence ν_E).

We have calculated tlie voltage across the cell using equation (3.14). The integration was performed by Simpson's rule. The voltage is 4.93 volt which is well above the expected Freedericksz threshold [$V_{th} \simeq \pi(K_{11}/\epsilon_o \Delta\epsilon)^{1/2}$] voltage of 3.95 volt.

In figures 3.4 we have plotted θ as a function of position across tlie cell thickness at three different times t= 0.225 T, 0.5 T, and 0.775 T within the period T for q = 300000 m^{-1}. The θ profile is found to be independent of both tlie sign and magnitude of q as is to be expected. Further, θ is symmetric about the centre of the cell. It does not change sign with time because θ oscillations arise due to the dielectric anisotropy of the sample and are quadratic in E. From equation (3.22) the dielectric torque is only a function of n_z and hence of only θ.

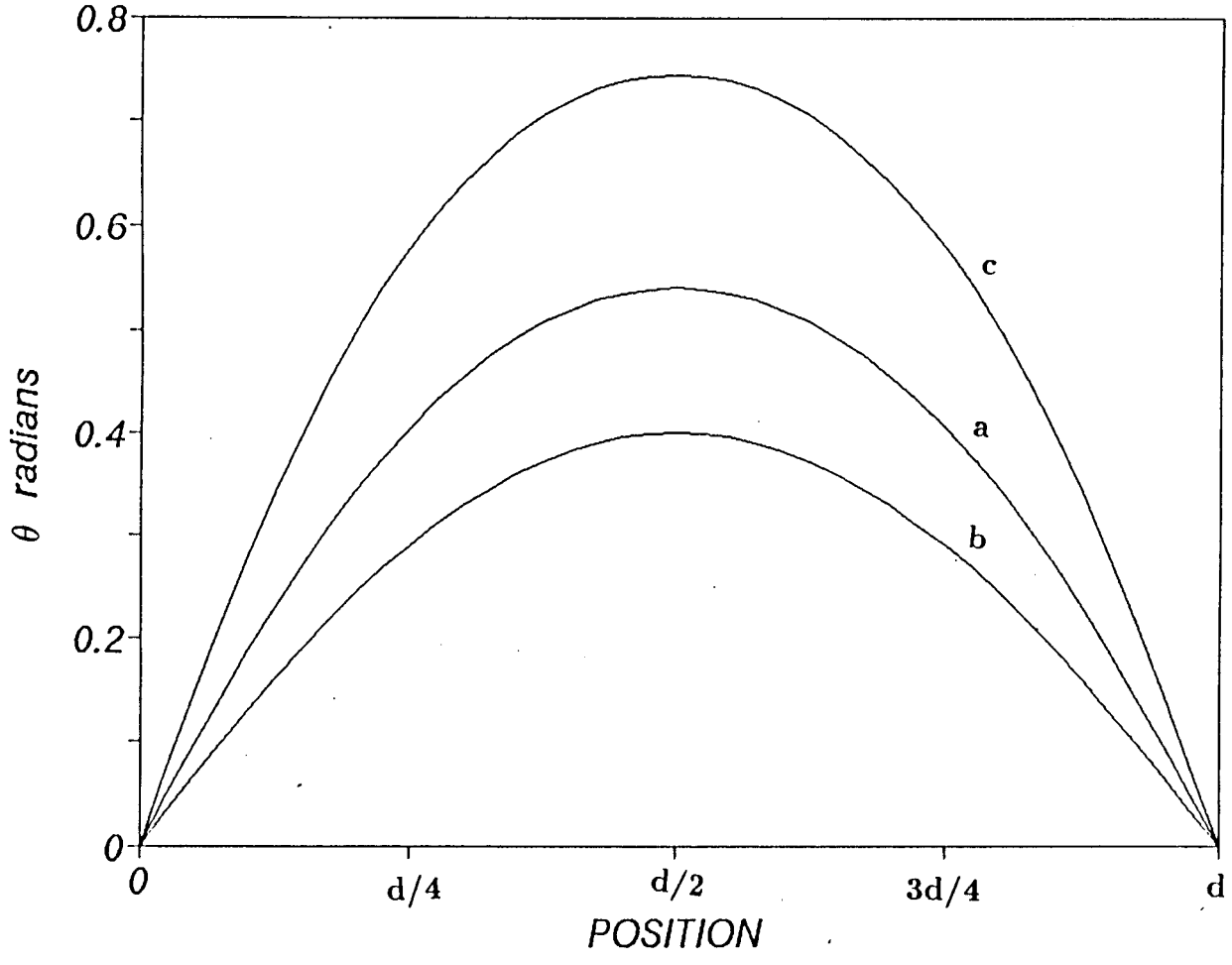

Figure 3.4. θ plotted as a function of position across the cell thickness at three different times. (a) t=0.225 T (b) 0.5 T and (c) 0.775 T for $q = 3 \times 10^5 m^{-1}$.

In figures 3.5 and 3.6 we have plotted the dependence of ϕ as a function of position across the cell calculated at the same times as in figure **3.4** and for . $q = 3 \times 10^5 m^{-1}$ and $q = -3 \times 10^5 m^{-1}$ respectively. The ϕ profile is asymmetric about the centre of the cell. This is due to the fact that the torques Γ_2 and Γ_3 depend linearly on $q \frac{\partial \phi}{\partial z}$ and $q \frac{\partial \theta}{\partial z}$ respectively [see equations **(3.34)** and **(3.35)).** The asymmetry changes sign during one period. This is because 4-oscillations which are caused by the electromechanical coupling are linear in E which changes sign with time. As the sign of q is changed, the sign of ϕ profile is also seen to change (see figures 3.5 and 3.6) as ν_E changes sign with that of q . In figure 3.7 ϕ has been plotted as a function of position at the same three relative times for $q = 1 \times 10^5 m^{-1}$. Comparing the profiles with those in figure 3.5, it is seen that as the q value is reduced by a factor of **3,** the 4-values have been reduced by the same factor, though the shape of the profile remains unaltered. This result also follows from our assumption that the electromechanical coupling coefficient is proportiorial to q .

We have also made calculations of the transmitted intensity as a function of time when such a sample is kept between crossed polarisers as shown in figure **3.3.** We assume that the angle made by the director at the lower plate with the polariser, $\psi_1 = \pi/8$ radians which maximises the signal due to ϕ oscillations as will be discussed in the next chapter. For this purpose, at any given instant of time in which $\theta(z)$ and $\phi(z)$ profiles are known, the calculations are made as follows.

Since both θ and ϕ vary with z in the nematic cell, the calculation of intensity should take into account both variations. For the purpose of calculation of optical transmission through the medium, we cut the sample into a number of slices of equal thickness Ad along the z axis. Then we calculate the phase acquired by the light beam passing through the slice, which depends on the local tilt angle θ. We assume

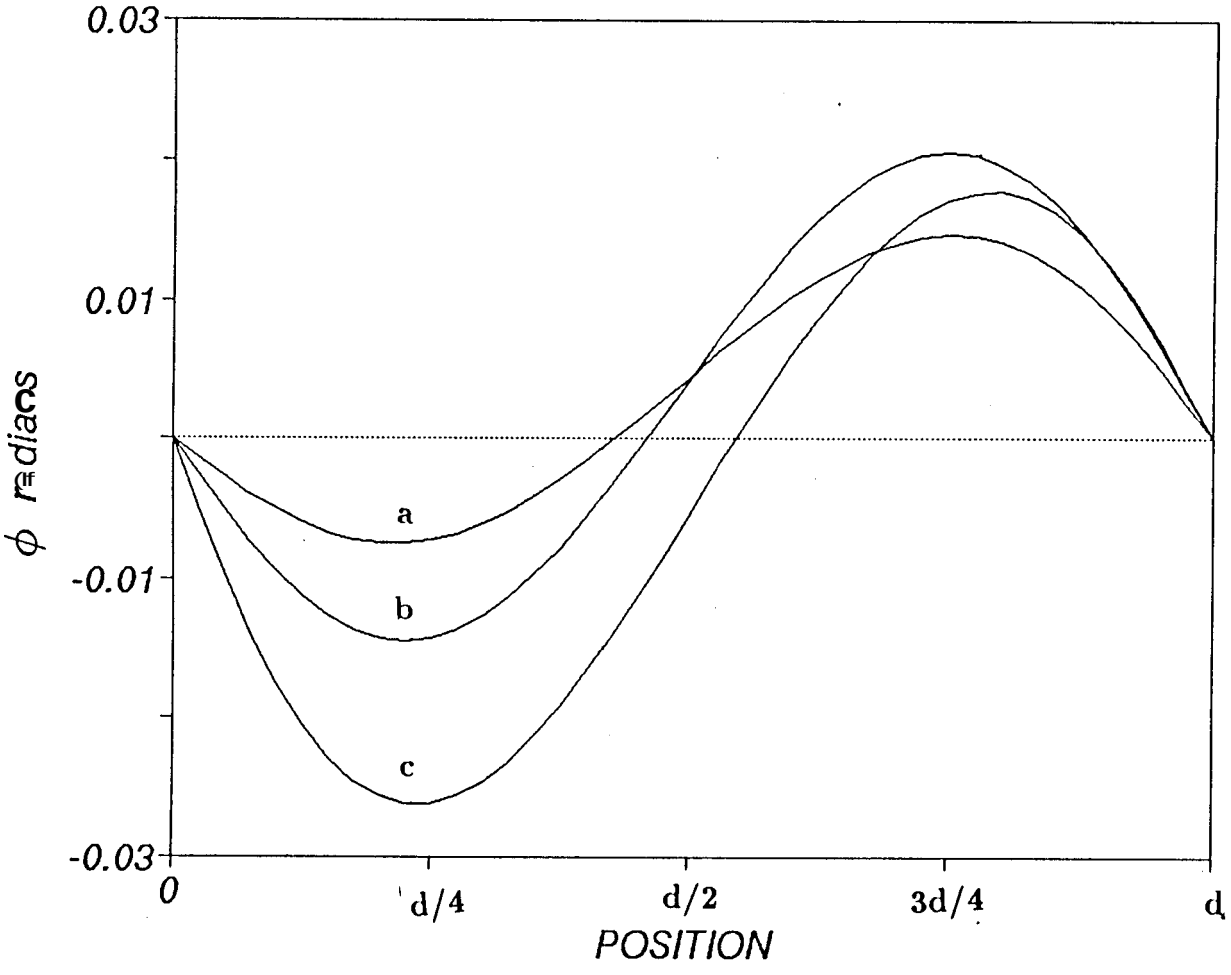

Figure 3.5. ϕ plotted as a function of position across the cell thickness at three different times. (a) $t=0.225$ T *(b) 0.5* T and *(c) 0.775* T for $q = +3\times10^{5}m^{-1}$.

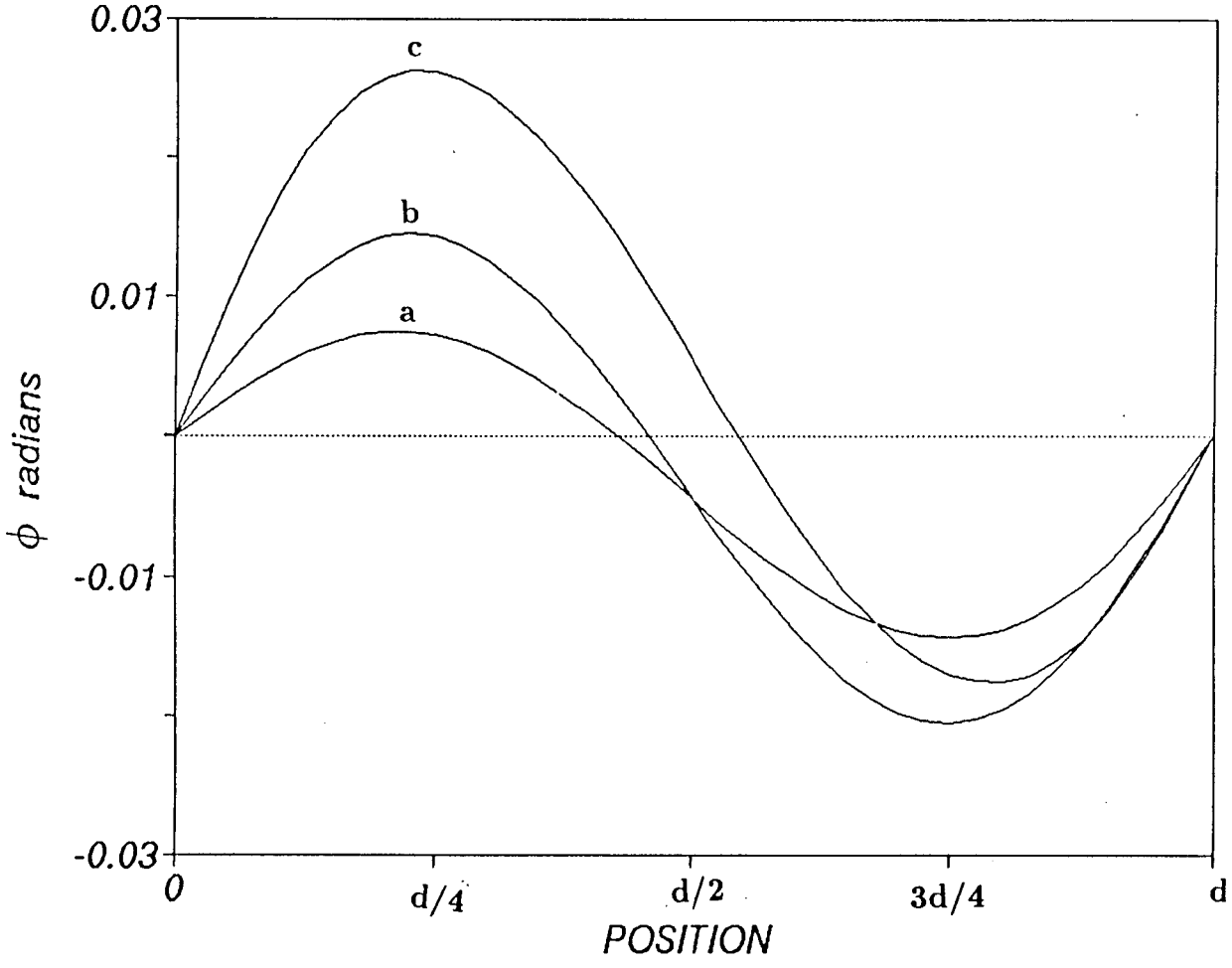

Figure 3.6. ϕ plotted as a function of position across the cell thickness at three different times. (a) t=0.225 T, (b) *0.5 T and (c) 0.775 T* for $q = -3\times10^{5}m^{-1}$.

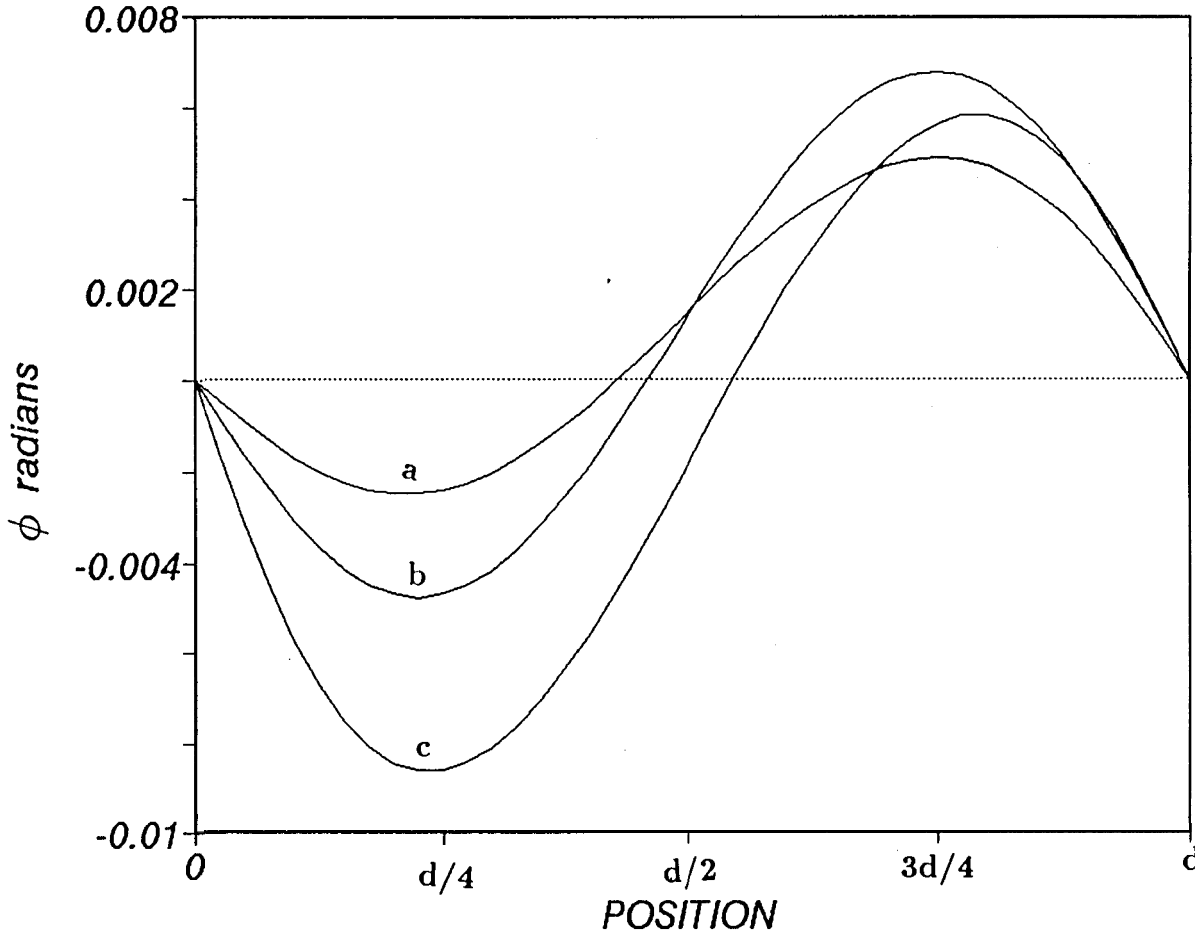

Figure 3.7. ϕ plotted as a function of position across the cell thickness at three different times. (a) t=0.225 T (b) *0.5* T and (c) 0.775 T for $q = 1\times10^{5}m^{-1}$.

each slice makes a uniform azimuthal angle ϕ, which is equal to that at the centre of the slice and a uniform tilt angle 8, which again corresponds to that at the centre of the cell.

Let ϕ_o be the angle between the polariser and $\vec{m}_1$, which is the projection of $\hat{n}$ at the centre of the first slice on the surface of the cell. Let E_o be the amplitude of the electric vector of the incident light beam at any given instant (Fig.3.8). Then the component of E_o along $\vec{m}_1$ is given by

$$E_{\|}^{in}(1) = E_o \cos\phi_o$$

and the component of E_o perpendicular to $\vec{m}_1$ is given by

$$E_{\perp}^{in}(1) = E_o \sin\phi_o \ .$$

Then the component of the field parallel to $\vec{m}_1$ after tlie light beam emerges from the first slice is (Fig.3.8)

$$E_{\|}^{o}(1) = E_{\|}^{in}(1)\, e^{i\alpha_1} \ .$$

Here α_1 is the phase angle acquired by the light beam and is given by

$$\alpha_1 = \frac{2\pi}{\lambda} n_{eff}\, \Delta d$$

where, $n_{eff} = (n_e n_o/(n_e^2 \sin^2\theta + n_o^2 \cos^2\theta)^{1/2}$.

Similarly tlie component orthogonal to $\vec{m}_1$ is given by $E_{\perp}^{o}(1) = E_{\perp}^{in}(1)\, e^{i\alpha_o}$ where $a, = \frac{2\pi}{\lambda} n_o \Delta d$. The components of the electric field of the light beam incident on the next slice are given by,

$$E_{\|}^{in}(2) = E_{\|}^{o}(1)\cos\Delta\phi_{12} + E_{\perp}^{o}(1)\sin\Delta\phi_{12}$$

$$\text{and} \quad E_{\perp}^{in}(2) = E_{\perp}^{o}(1)\cos\Delta\phi_{12} - E_{\|}^{o}(1)\sin\Delta\phi_{12}$$

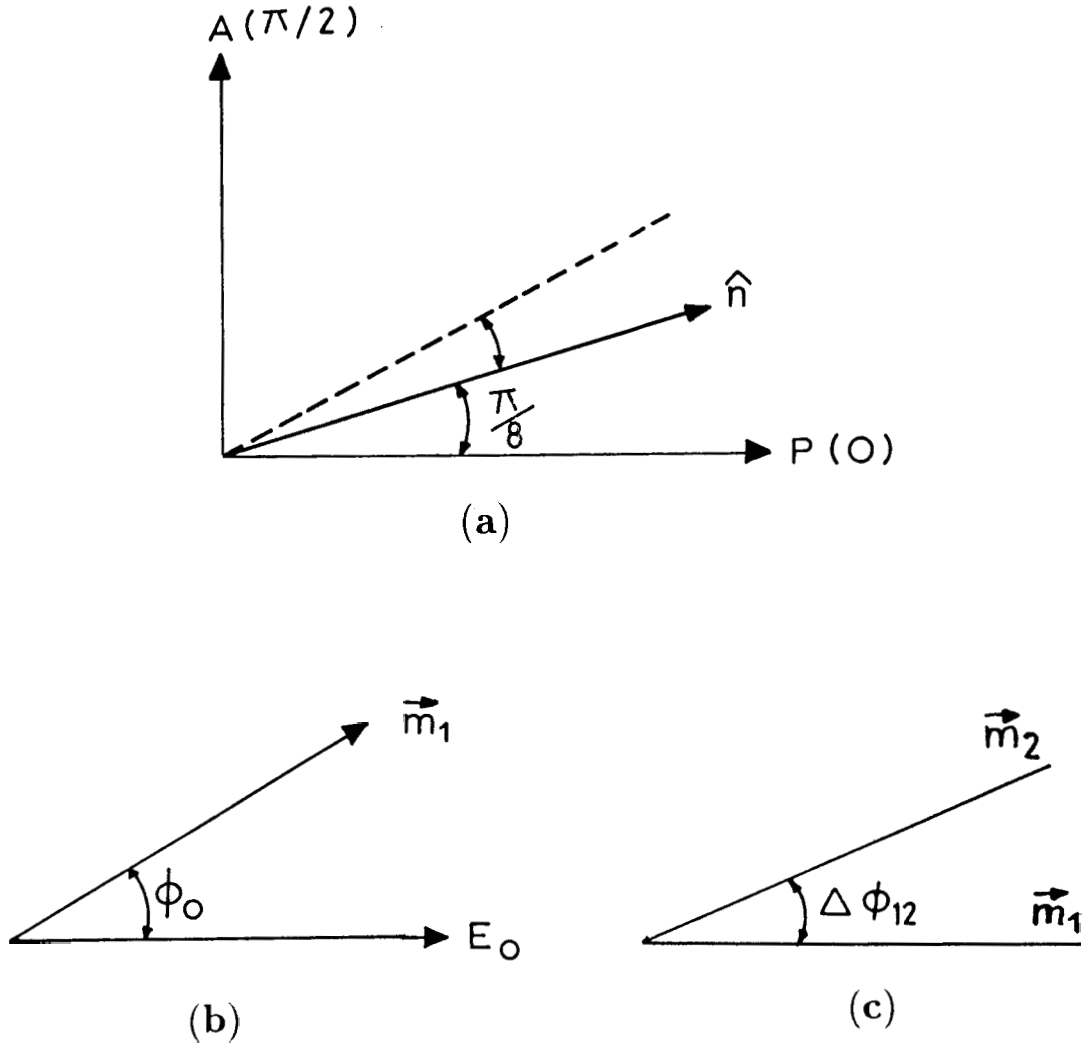

Figure 3.8. (a) P is the polarizer, A is tlie analyses, $\hat{n}$ is the nematic director at tlie lower plate and tlie dotted line represents tlie projection of $\hat{n}$ at tlie upper plate; (I)) m_1 is the projection of the director in the centre of the first slice on the XY plane. E_o is tlie amplitude of the electric vector of the incident light beam. (c) ı and $\vec{m}_2$ are tlie projections of tlie director at the centres of first and second slices respectively on the XY plane.

where $\Delta\phi_{12}$ is the angle made by the projection of the director at the centre of the second slice on the XY plane, i.e., $\vec{m}_2$ with $\vec{m}_1$ (Fig.3.8).

After passing through the second slice the electric field components are given by

$$E_{\|}^{o}(2) = E_{\|}^{in}(2)\, e^{i\alpha_2} \text{ and } E_{\perp}^{o}(2) = E_{\perp}^{in}(2)\, e^{i\alpha_o}.$$

Continuing the calculations in the same way the light beam coming from the last, i.e., N^{th} slice has the components of the field given by

$$\begin{aligned} E_{\|}^{o}(N) &= E_{\|}^{in}(N-1)\, e^{i\alpha_N} \text{ parallel to } \vec{m}_N \text{ and} \\ E_{\perp}^{o}(N) &= E_{\perp}^{in}(N-1)\, e^{i\alpha_o} \text{ perpendicular to } \vec{m}_N. \end{aligned}$$

Therefore the resultant electric field of the emergent light beam is given by,

$$E^o = E_{\|}^{o}(N)\cos\phi_1 + E_{\perp}^{o}(N)\sin\phi_1$$

where ϕ_1 is the azimuthal angle between the analyser (which is crossed with respect to the polariser) and $\vec{m}_N$.

The intensity of the emergent light is given by

$$I^o = E^o E^{o*} = |\, E^o\,|^2 ,$$

where E^{o*} is the complex conjugate of E^o.

I^o is shown as a furiction of time in figure 3.9 for $q = +3\times10^5 m^{-1}$. The intensity has two nearly equal peaks within the time period, showing that the 2f-component due to 0-oscillations make the dominating contribution. However, there is a clear phase difference between θ and E oscillations, as can be expected from a viscous systern. We may also note that the second peak is slightly lower than the first one showing that there is an 1f component which arises from the electromechariical coupling. Indeed the time-dependence of the intensity for $q = -3\times10^5 m^{-1}$ shown in

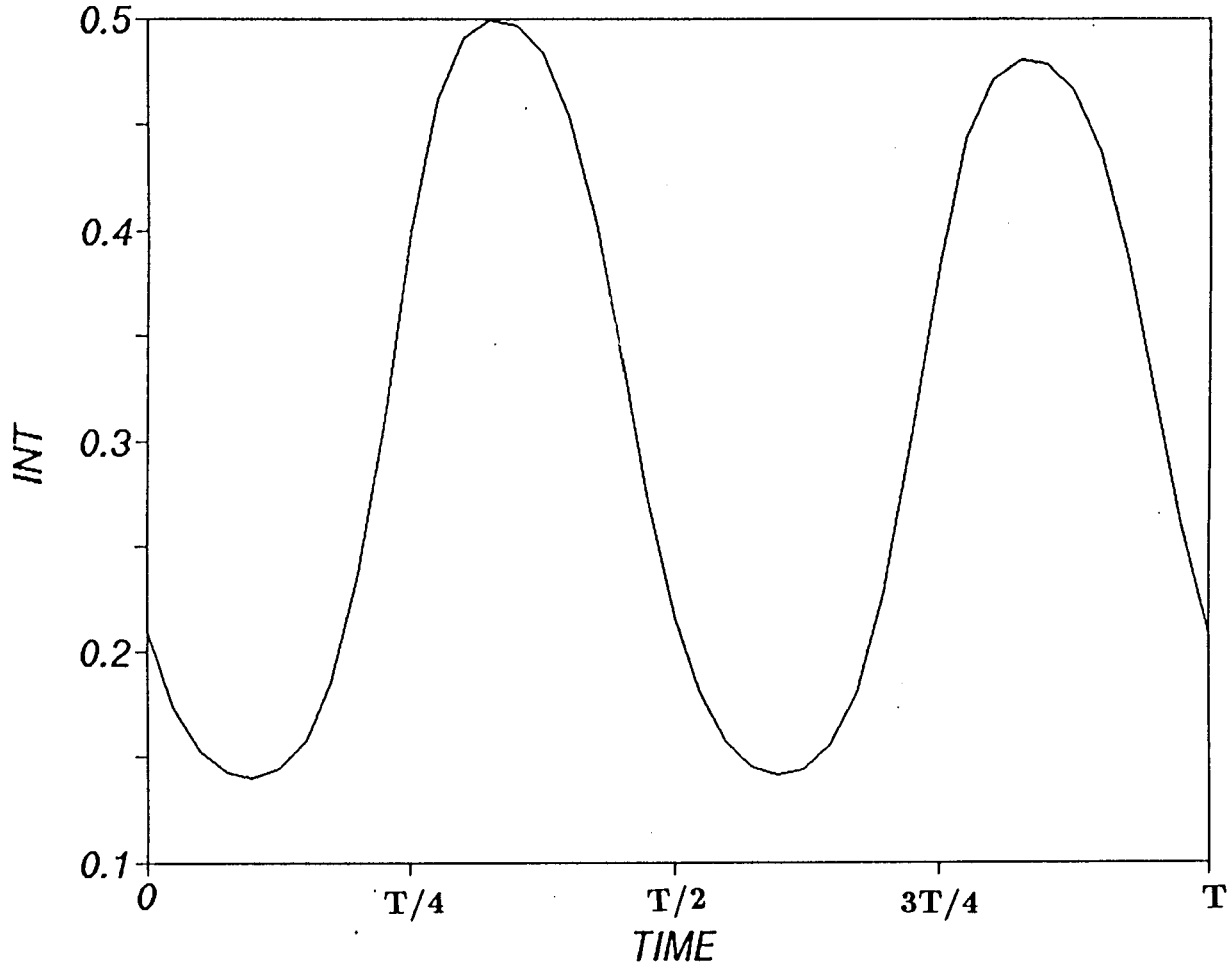

Figure 3.9. Intensity of transmitted light plotted as a functiori of time for q = $+3\times10^{5}m^{-1}$.

figure 3.10 has the opposite trend: the first peak is lower than the second one as is to be expected.

We have calculated the DC, $1f$ and $2f$ components of the intensity of light by calculating the appropriate Fourier components as follows:

$$
\begin{aligned}
I_o &= \frac{1}{T}\int_o^T I(t)\,\mathrm{dt} \\
I_{1f}(i) &= \frac{2}{T}\int_o^T I(t)\sin\, wt\, dt \\
I_{2f}(\mathrm{i}) &= \frac{2}{T}\int_o^T I(t)\sin\, 2\omega t\, dt \\
I_{1f}(o) &= \frac{2}{T}\int_o^T I(t)\cos\,\omega t\,\mathrm{dt} \\
I_{2f}(o) &= \frac{2}{T}\int_o^T I(t)\cos\, 2\omega t\, dt
\end{aligned}
$$

where $I_{1f}(\mathrm{i})$ and $I_{1f}(o)$ are the components of intensity of the transmitted light in phase and $\pi/2$ out of phase with the applied electric field $\mathrm{E} = E_o e^{i\omega t}$ etc. The absolute values of the intensity are given by

$$
\begin{aligned}
|\, I_{1f}\,| &= \sqrt{I_{1f}^2(i) + I_{1f}^2(o)} \\
|\, I_{2f}\,| &= \sqrt{I_{2f}^2(i) + I_{2f}^2(o)}
\end{aligned}
$$

As can be expected, I, and $|\, I_{2f}\,|$ are practically independent of the sign of q. On the other hand, the phase of I_{1f} changes when q is reversed. We have calculated I_{1f} as a function of q for $D_{zo} = 9.36\times10^6 V/m$. The results are shown in figure 3.11. The calculated magnitude of the intensity for a given value of $+q$ is greater than that for $-q$. This may arise from the small number of slices (41) used in the calculations. The sign of the phase however changes when the sign of q changes. We could not explore values of q close to zero as the computer time became prohibitively long.

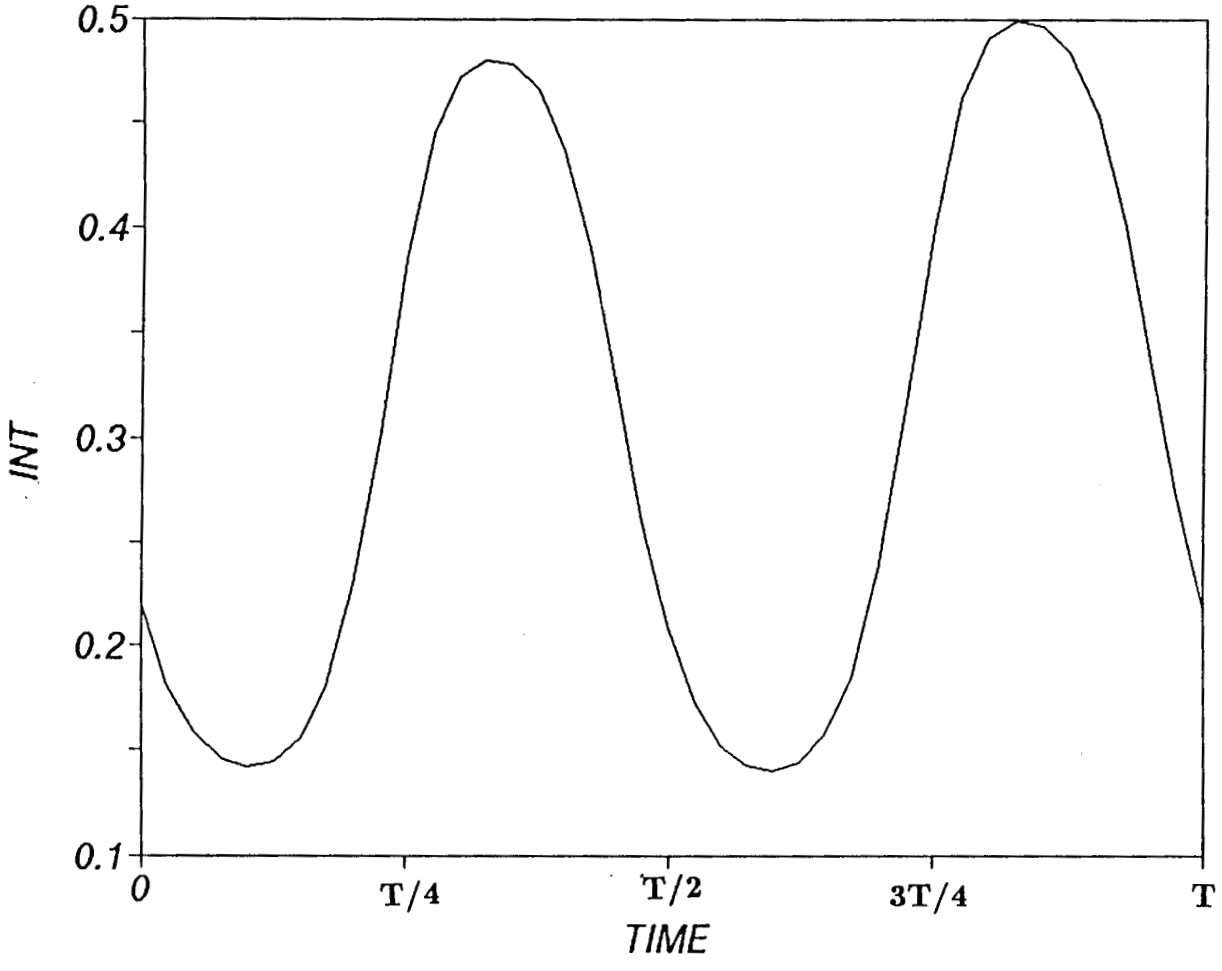

Figure 3.10. Intensity of transmitted light plotted as a function of time for $q = -3\times10^{5}m^{-1}$.

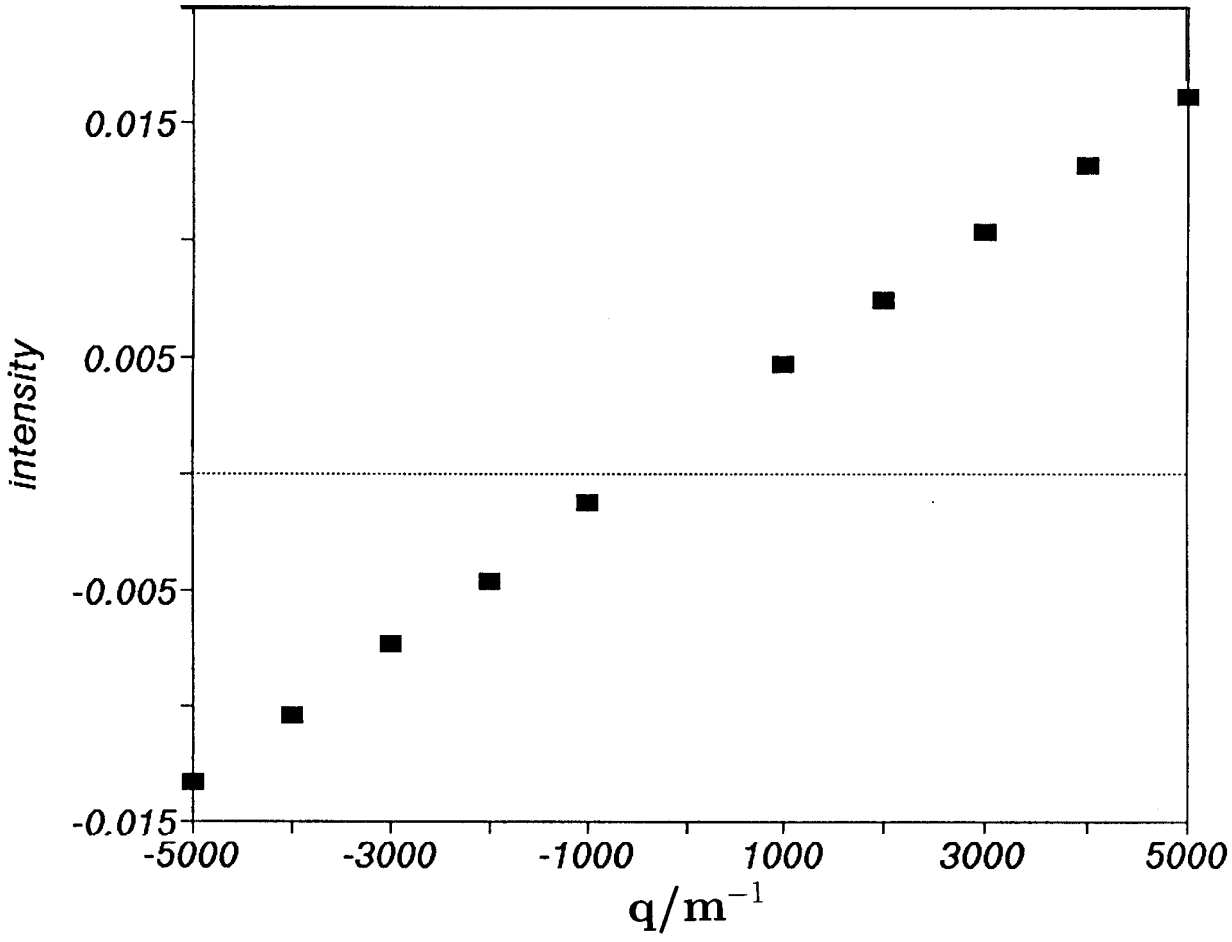

Figure 3.11. The plot of I_{1f} versus q for $D_{zo} = 9.36\times10^{6} Vm^{-1}$

We describe in the next chapter our experimental studies on the electromechanical effect in samples with fixed boundary conditioris in cliolesteric liquid crystalline mixtures with a negative dielectric anisotropy using conoscopy. We have also made measurements on samples with positive dielectric anisotropy.

REFERENCES

BOBYLEV,Yu.P., and PIKIN,S.A., 1977, *Sov.* Phys. JETP, **45**, 195.

BODENSCHATZ,E., ZIMMERMANN,W., and KRAMER,L., 1988, J. Phys. France, 49, 1875.

CHIGRINOV,V.G., BELYAEV,V.V., BELYAEV,S.V., and GREBENKIN,M.F., 1979, *Sov.* Phys. JETP, 50, 994.

DE GENNES,P.G., 1975, The Physics *of* Liquid Crystals, Clarendon Press.

LESLIE,F.M., 1968, Proc. Roy. *Soc.,* London, **A307**, 359.

LESLIE,F.M., 1971, in Advances in Liquid Crystals, Vol.4, Ed. G.H.Brown, p.1.

MADHUSUDANA,N.V., and PRATIBHA,R., 1989, Liquid Crystals, 5, 1827.